



Thermal Vacuum 2: measures of the IR background and on-orbit predictions (SMS IR01S18).

M. Robberto
July 15, 2008

Abstract

The total background flux seen by the WFC3-IR detector has been measured during the June-August 2007 Thermal Vacuum 2 (TV2) Campaign. The measured values agree within ~10% with our model. We predict the thermal background that will be seen on orbit with both the current (FPA129) and next (FPA165) IR FPAs, showing that it will fall well within the 0.4e/s limit stated by the CEI specification document, including detector the dark current (peak value). We also verify the general compliance of WFC3 estimated background with all relevant CEI specifications.

1. Introduction

During the Thermal Vacuum 2 Campaign held at Goddard in June-August 2007, a sequence of measures (SMS-IR01S18) has been performed to verify the amount of thermal flux seen by the WFC3-IR FPA in all filters. The same sequence had been previously executed in the 2004 Thermal Vacuum (TV1) campaign. At that time, it revealed two unexpected anomalies: 1) a periodic oscillation of the dark current level, and 2) and exceedingly high background in the G141 grism (Hilbert & Robberto 2005). Fixes to these problems have been put in place between the two TV campaigns, respectively with a redesign of the circuitry controlling the FPA temperature, and with the addition of an IR coating on the G141 grism closely matching the F140W bandpass. In TV2 this SMS was therefore repeated to validate the successful solution of both problems.

Renewed interest in this SMS was also originated by the availability of new IR FPAs characterized by higher quantum efficiency. In particular, the strong candidate FPA165 has a potential flaw in its redder long wavelength cutoff. This causes an increase of the background flux seen in all filters. To estimate the increase of background one has to use a rather detailed model, since the QE drops to zero in a region where the various sources of background rise exponentially. If the model can predict the thermal background seen with the FPA129 in TV2, then the estimate for FPA165 are also reliable.

2. Data acquisition and analysis

The SMS-IR01S18 was run on July 2nd, 2007 with the instrument running on side-2 electronics. The SMS cycles through the entire set of filters, interleaving a ramp taken with the blank filter in (i.e. a real dark) with a ramp taken through a filter with all lights in the vacuum chamber turned off. In this way, the only signal entering through the filter is the thermal radiation from the environment, which is expected to be significant at the longest wavelengths. The ramps are taken in SPARS100 mode stopped after the 4th read, for a total integration time of 202.9s.

The data have been reduced using an IDL procedure developed for quick look of the IR images taken during thermal vacuum. The procedure subtracts from each read the average value of the onboard vertical reference pixels and estimate a robust-mean value with an iterative sigma clipping algorithm; it then produces a linear fit to the signal accumulated by each pixel, estimating the average dark current (from the slope of the linear fit), the bias (from the intercept) and the readout noise (from the variance around the fit, taking into account the two degrees of freedom taken by the linear fit). The dark current, bias and readout noise maps are therefore analyzed with a routine fitting a gaussian profile to the histograms. The mean values of the gaussian fit are the numbers reported here. A typical output of the IDL routine is presented in Figure 1.

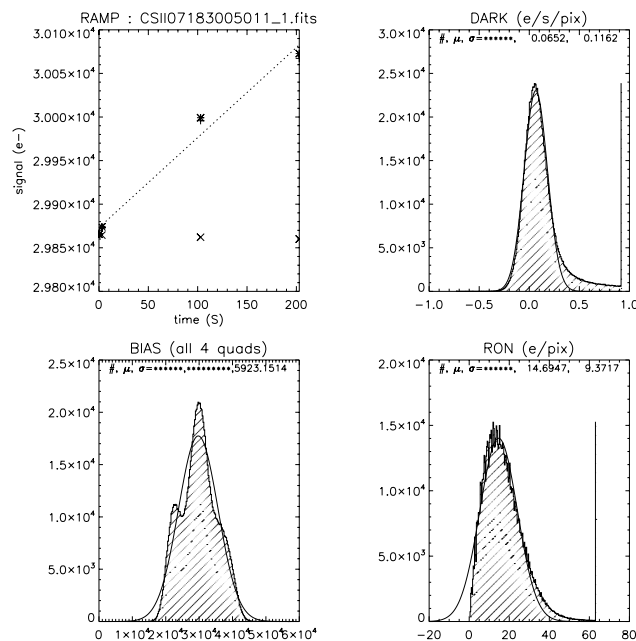


Figure 1: output of the IDL quick look routine: top-left) dark current ramp. The “x” signs indicate the reference pixels. ; top-right) dark current histogram; bottom-left) bias histogram; bottom-right) readout noise histogram.

Figure 1 shows that the dark (top-left plot) does not increase linearly with time, as predicted by theory (Robberto & Hilbert, 2005). It also show the significant tail of hot pixels in the dark current rate histogram (top-right plot), the quadrant to quadrant electronic offset (bottom-left plot), and the distribution of the single-read readout noise (bottom-right plot). This last value has to be multiplied by $\sqrt{2}$ to produce the double correlated sampling noise usually quoted. Note that the non linearity of the dark current produces an overestimate of the readout noise.

Table 1 shows a log of the SMS with the dark current rates obtained for each ramp. The results are also plotted in Figure 1.

TABLE 1

<i>Entry</i>	<i>file</i>	<i>Filter</i>	<i>counts(e/s)</i>
32334	CSII07183005011_1.fits	Blank	0.0652
32335	CSII07183005414_1.fits	F098M	0.0634
32336	CSII07183005814_1.fits	Blank	0.0656
32337	CSII07183010215_1.fits	F105W	0.0358
32338	CSII07183010613_1.fits	Blank	0.0387
32339	CSII07183011012_1.fits	F110W	0.0352
32340	CSII07183011407_1.fits	Blank	0.0346
32341	CSII07183011802_1.fits	F125W	0.0304
32342	CSII07183012158_1.fits	Blank	0.0337
32343	CSII07183012555_1.fits	F126N	0.03
32344	CSII07183012959_1.fits	Blank	0.0365
32345	CSII07183013403_1.fits	F127M	0.031
32346	CSII07183013806_1.fits	Blank	0.0373
32347	CSII07183014208_1.fits	F128N	0.0319
32348	CSII07183014609_1.fits	Blank	0.0388
32349	CSII07183015009_1.fits	F130N	0.0317
32350	CSII07183015408_1.fits	Blank	0.0411
32351	CSII07183015806_1.fits	F132N	0.0358
32352	CSII07183020212_1.fits	Blank	0.0429
32353	CSII07183020618_1.fits	F139M	0.0347
32354	CSII07183021024_1.fits	Blank	0.0428
32355	CSII07183021430_1.fits	F140W	0.1354
32356	CSII07183021838_1.fits	Blank	0.0409
32357	CSII07183022246_1.fits	F153M	0.0789
32358	CSII07183022639_1.fits	Blank	0.0433
32359	CSII07183023031_1.fits	F164N	0.1234
32360	CSII07183023426_1.fits	Blank	0.0452
32361	CSII07183023821_1.fits	F167N	0.1694
32362	CSII07183024214_1.fits	Blank	0.0443
32363	CSII07183024607_1.fits	F160W	0.5539
32364	CSII07183025011_1.fits	Blank	0.0444
32365	CSII07183025415_1.fits	G102	0.0379
32366	CSII07183025812_1.fits	Blank	0.0457
32367	CSII07183030209_1.fits	G141	0.4496
32368	CSII07183030641_1.fits	Blank	0.0431

3. Results

The mean dark current rates reported in Table 1 are also plotted in Fig. 2 and, with a different scale, in Fig. 3.

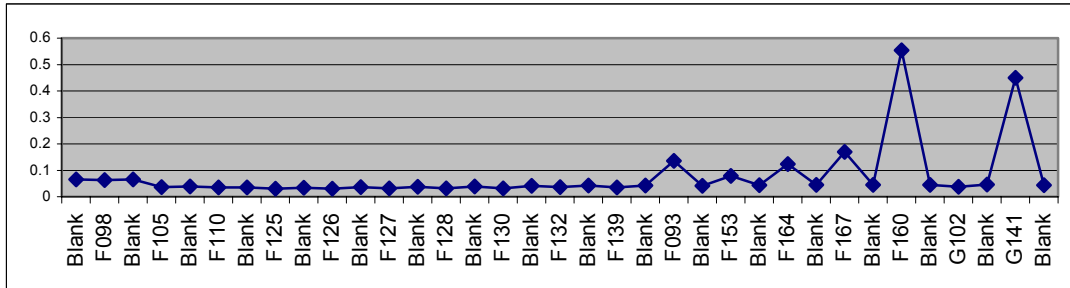


Figure 1: mean dark current recorded during the execution of the SMS-IR01S18.

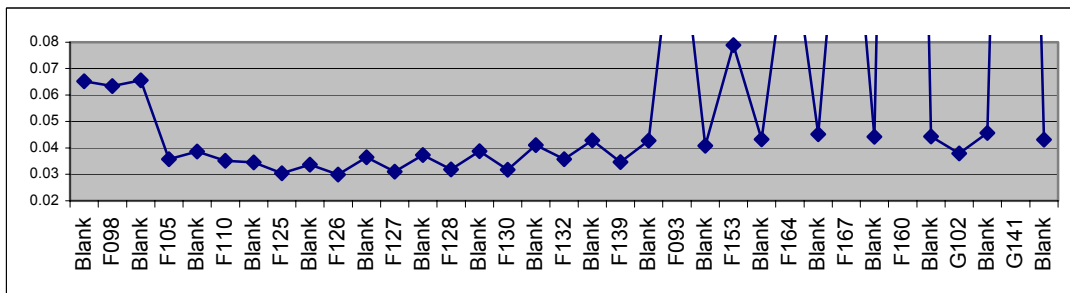


Figure 1: same as Figure 2, scaled to illustrate the variations at the lowest dark levels.

As expected, the dark current is generally low for the “blue” filters and increases in the filters with a redder bandpass, reaching the maximum values in the F160W and G141 grism. Note that the grism has a lower rate than the F160W, it was approximately 3 times higher in the TV1 campaign, as a result of the application of the additional AR coating. The high signal seen in the first 3 ramps is probably related to an initial thermal instability of the detector and will be ignored in our analysis.

An interesting phenomenon is the increase of dark current when the blank is inserted in the filter wheel instead of a filter (evident in Figure 3). This is due to the fact that even if both element are opaque (of course, out of the transmission window for the filter), the blank has always emissivity close to 1 whereas the filters are partially reflecting. Since the side facing the detector reflects a colder environment, the total emission of the filters is lower than that of the blank.

4. Model predictions

The dark current measured in the F160W filter and G141 grism is higher than the total dark current signal allowed in the CEIS document, 0.4 e/s/pixel. However, the thermal background in the thermal vacuum chamber is higher than that expected on-orbit, so this may not be represent a problem. This can be confirmed using a model developed to predict the background seen by WFC3 in both environments, described in detail in Robberto (2003)

For this study, we have considered two detectors: FPA129, used in TV2 to collect the data presented in this document, and FPA165, selected for WFC3-IR build 4 and the most viable candidate as final WFC3-IR flight detector. Their quantum efficiency curves are presented in Figure 4. Note that both curves represent values corrected for intra-pixel capacitive coupling.

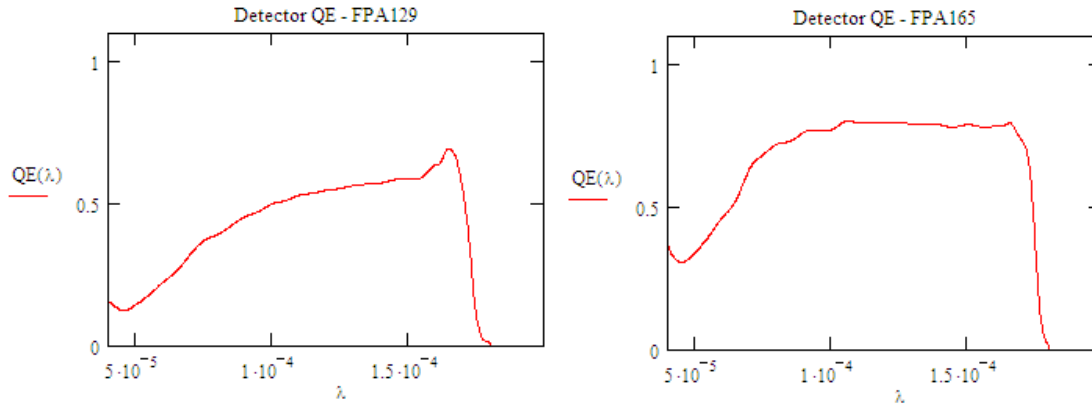


Figure 4: quantum efficiency curves for the FPA129 and FPA165 detectors.

The temperatures we have assumed for the cold enclosure and inner shield are those provided by the WFC3 telemetry during the execution of the SMS and are rather typical. For the cold enclosure (which is also the temperature of the filter elements) we have used -45 C, for the inner radiation shield we used -85 C (sides) and -92.5 C (top). These last two temperatures are very low and, despite the large solid angle subtended by these surfaces as seen by the detector, contribute negligibly to the thermal background. For the thermal vacuum chamber we have used +14.4 C, also measured during the tests; this will be the temperature of the thermal bath seen by the detector through the filter.

The detector has an intrinsic dark current which is not included in our thermal model. The intrinsic dark current cannot be higher than the minimal dark current seen when the blue filters are inserted, approximately 0.03e/s. We assume for simplicity that the dark current accounts exactly for this value, i.e. DC=0.03e/s.

As we already mentioned, the decrease of dark signal when the blue filters are inserted suggests that we are overestimating the off-band emissivity of the filters. We can use the difference between filters and blank to estimate the filter reflectivity. This is basically the same principle of IR reflectometers, that measure reflectance of materials at known temperatures to derive their emissivity. We will assume an off-band filter emissivity of 10% and a corresponding 90% reflectivity of a blackbody at -60C. We underline that these values are inserted to explain the background seen in the blue filters, and should be taken only as a first approximation.

Using the parameters listed above, we obtain the results presented in Table 2.

TABLE 2 – TV 2 prediction vs. measure

Filter	Model	Model + DC	TV2 Measure
DARK:	0.007 e/s	0.037 e/s	0.043 e/s
F126N:	0.001 e/s	0.031 e/s	0.030 e/s
F153M:	0.046 e/s	0.076 e/s	0.079 e/s
F164N:	0.095 e/s	0.125 e/s	0.123 e/s
F167N:	0.133 e/s	0.163 e/s	0.152 e/s
F160W:	0.516 e/s	0.546 e/s	0.554 e/s
G141	0.469 e/s	0.499 e/s	0.450 e/s

In general, our predictions are within 10% of the measured rates. Given the uncertainties on the measures (our quick look estimator is slightly biased toward higher values due to the presence of the hot pixel tail), and of the model (which does not take into account diffraction effects at the pupil that blur the hot and warm part of the beam) we regard this agreement as quite satisfactory.

4. Predictions for WFC3 on orbit.

Having successfully validated (within ~10%) our model, we can now predict the thermal background that will be seen on-orbit, in different filters. Again, we use the same method described by Roberto (2003), with a temperature of -45C for the filter and cold enclosure.

Table 3 shows the results of our calculation for FPA129 and FPA165 without adding the dark current contribution.

TABLE 3 – FPA 129 vs. FPA165 on orbit

Filter	FPA129	FPA 165
F126N:	0.0014 e/s	0.0024 e/s
F153M:	0.0066 e/s	0.0095 e/s
F164N:	0.012 e/s	0.015 e/s
F167N:	0.017 e/s	0.020 e/s
F160W:	0.062 e/s	0.075 e/s
G141	0.056 e/s	0.070 e/s

If we add to these values a nominal 0.03 e/s of dark current we estimate for FPA129 and 0.022 for FPA165 gives values of ~0.1 e/s or less, well below the 0.4e/s allocated in the CEI Specification document.

4. Comparison with CEI Specifications

In this section we use our model to assess the compliance of WFC3, with the FPA 165 detectors, with the various CEI Specifications relative to the IR background contribution. There are 5 relevant requirements, listed in Table 4:

TABLE 4 – CEI Specifications relative to the IR background signal

Req. Number	Topic	Specification
4.4.8.1	IR Total Background Signal	The combined HgCdTe detector dark current and signal from radiation generated internal to the WFC3 and HST shall not exceed 0.4 electrons/pixel/second at the nominal operating temperatures with a goal of 0.1 electrons/pixel/second in any filter. This specification does not include the emission contribution from the amplifiers on the detector.
4.4.8.4	IR Background Signal Housing Contribution Limit	The IR Channel background contribution from the cold optical baffle and detector housing window shall not exceed 0.01 electrons per pixel per second with the cold optical baffle at a nominal operating temperature of -80 degrees C, and the detector housing window at a nominal operating temperature of -30C degrees C.
4.4.8.5	IR Background Signal Housing Channel filters and Cold Optics Limit	The IR Channel background contribution from the IR Channel filters and any optics (including the Refractive Corrector Plate) in the Cold Enclosure shall not exceed 0.02 electrons per pixel with the Cold Enclosure at a nominal operating temperature of -30 degrees C.
4.4.8.6	IR Background Signal Cold Optics Contribution Limit	The IR Channel background contribution from the IR Channel warm optics and the WFC3 pickoff mirror shall not exceed 0.08 electrons per pixel per second at a nominal operating temperature of 0 degrees C for the WFC3 optics and 14.6 degrees C for the pickoff mirror.
4.4.8.7	IR Background Signal OTA Optics and WFC3 Pupil Cold Mask Contribution Limit	The IR Channel background contribution from the HST OTA shall not exceed 0.11 electrons per pixel per second at a nominal operating temperature of -30C for the IR Channel Cold Mask, and assuming 15C for the OTA primary mirror and 17C for the OTA secondary mirror.

Here are our findings:

1. Requirement 4.4.8.1, on the IR Total background has been already addressed in the previous section, where we have shown that it is verified in all representative filters.
2. Requirement 4.4.8.4, on the IR background produced by the detector housing, can be verified by adding the signal coming from the walls and top of the cold enclosure and through the outer parts of the filter which see warm emission from the detector enclosure. This last contribution is larger for the F160W filter. In this case, it is $N=0.0049e/s$, which is approximately half the specified value.
3. Requirement 4.4.8.5, on the IR background produced by the filter and cold optics is detector housing, can be verified by estimating only the signal coming through the filter, setting to zero the background signal coming from the WFC3 optics, HST

OTA and zodiacal light. In this case, it is $N=1.7 \times 10^{-4}$ e/s for the F110W filter (this is the highest because the filter has emissivity=1 at long wavelengths, where its transmission drops to zero), which is approximately 1% of the specified value.

4. Requirement 4.4.8.6, on the IR background produced by the WFC3 optics (note that these are “warm” optics, i.e. the “cold” in the Topic description is a typo), including pick the pick-off mirror, can be verified by estimating the signal coming through the F160W filter, neglecting the telescope OTA and zodiacal light. It is $N=0.021$ e/s, where we have included the negligible contribution from the RCP and filter transmission curve since a white light estimate is not relevant. This value is 4 times lower than the specified value.
5. Requirement 4.4.8.6, on the IR background produced by the HST OTA can be estimated by neglecting the modulation produced by the WFC3 warm optics. It results, for the F160W filter and including the cold RCP and filter, $N=0.042$ e/s, which is approximately 3 times lower than the specified value.

5. Conclusion

We have measured the thermal background seen by the WFC3-IR FPA129 detector in Thermal Vacuum 2 2007 campaign and compared it with our model, assuming the temperatures for the cold enclosure, radiation shield and vacuum chamber measured during the test. The agreement is generally within 10%. We have then estimated the background signal expected for both FPA129 and FPA165 on orbit, finding values of ~ 0.1 e/s/ or less, including 0.03 e/s of nominal dark current. This is well below the original CEI specifications of 0.4 e/s/pix. We have also verified the general compliance of WFC3 estimated background with all relevant CEI specs.

References

Robberto, M. & Hilbert, B. 2005, “WFC3 2004 Thermal Vacuum Campaign: IR channel linearity (flat field illumination - SMS IR04)”, WFC3 ISR 2005-29

B. Hilbert & M. Robberto, 2005, “WFC3-IR Thermal Vacuum Testing: IR Channel Dark Current”, WFC3 ISR 2005-25

M. Robberto 2003, “Model of thermal background at the focal plane of the WFC3-IR channel”, WFC3 ISR 2003-09